Journal of Thermal Biology 98 (2021) 102932

Contents lists available at ScienceDirect

Journal of Thermal Biology

journal homepage: http://www.elsevier.com/locate/jtherbio

Thermal radiation management by natural photonic structures: *Morimus asper funereus* case

Darko Vasiljević [a], Danica Pavlović [a,*], Vladimir Lazović [a], Branko Kolarić [a,c], Branislav Salatić [a], Wang Zhang [b], Di Zhang [b], Dejan Pantelić [a]

[a] Institute of Physics, University of Belgrade, Pregrevica 118, 11080, Belgrade, Zemun, Serbia
[b] State Key Lab of Metal Matrix Composite, Shanghai Jiao Tong University, 800 Dongchuan Road, Shanghai, 200240, China
[c] Micro- and Nanophotonic Materials Group, University of Mons, Place du Parc 20, 7000, Mons, Belgium

ARTICLE INFO

Keywords:
Photonic structures
Infrared radiation
Hyperuniformity
Radiative energy exchange
Longicorn beetle

ABSTRACT

Convective, conductive and radiative mechanisms of thermal management are extremely important for life. Photonic structures, used to detect infrared radiation (IR) and enhance radiative energy exchange, were observed in a number of organisms. Here we report on sophisticated radiative mechanisms used by *Morimus asper funereus*, a longicorn beetle whose elytra possess a suitably aligned array of lenslets and blackbodies. Additionally, a dense array of microtrichia hyperuniformly covers blackbodies and operates as a stochastic, full-bandgap, IR-photonic structure. All these features, whose characteristic dimensions cover a range from several hundred down to a few micrometres, operate synergistically to improve the absorption, emission and, possibly, detection of IR radiation. We present a morphological characterization of the elytron, thermal imaging measurements and a theoretical IR model of insect elytron, uncovering a synergistic operation of all structures.

1. Introduction

Colouration in the living world serves multiple purposes, such as: camouflage, mimicry, warning or attraction (Doucet and Meadows, 2009; Kemp, 2007; Sweeney et al., 2003; Verstraete et al., 2019), and it sometimes affects the very existence of animals. Radiative heat exchange with the environment can also be influenced by colours, through absorption or reflection of the visible light. There is a delicate balance between colouration and other mechanisms of thermal regulation: convection, conduction, radiation emission and absorption, evaporation, perspiration, internal heat generation, behaviour (Bosi et al., 2008; Cossins, 2012).

Such mechanisms have also been observed in insects. Their exoskeleton (cuticle) serves many functions, such as: locomotion, providing a defence barrier (against mechanical stress, cold, hot or wet environment), a reservoir for the storage of metabolic waste products, mechano- and chemoreception, balancing radiant energy absorption in the visible and dissipation in the infrared (IR) part of the spectrum (Capinera, 2008; Gillott, 2005; Gullan and Cranston, 2004; Shi et al., 2015). The cuticle is usually patterned on micro- and nano-scale and produces striking optical effects. Such photonic structures (Vukusic and Sambles, 2003) create structural colouration (Vukusic et al., 2001) in the visible, but can have an important role in the infrared part of the spectrum, participating in thermoregulation (Scoble, 1992; Shi et al., 2015).

Most insects are primarily ectothermic and rely on external heat sources, such as solar radiation (Nijhout, 1991). It is proven that butterflies use physiological mechanisms to regulate the heat gain by orientation and posture relative to the sun (Kingsolver, 1985). On the other hand, structures are developed during evolution to efficiently reflect the visible light, simultaneously dissipating infrared radiation directly into the atmospheric window at mid-infrared, as in the Saharan silver ant, *Cataglyphis bombycina* (Roger, 1859) (Shi et al., 2015). This clever mechanism enables an insect to efficiently regulate its body temperature in a hostile desert environment.

In addition, the insect cuticle can be a place where so-called extraocular photoreception occurs. Also known as “dermal light sense” and defined as a “widespread photic sense that is not mediated by eyes or eyespots and in which light does not act directly on an effector” (Millott, 1968), it has been reported in several orders of insects. Some butterflies have such photoreceptors located at the end of their abdomens to control copulation in males and oviposition in females (Arikawa and Takagi,

* Corresponding author. Institute of Physics, University of Belgrade, Serbia Pregrevica 118, 11080, Belgrade, Zemun, Serbia.
E-mail address: danica.pavlovic@ipb.ac.rs (D. Pavlović).

https://doi.org/10.1016/j.jtherbio.2021.102932
Received 19 November 2020; Received in revised form 5 March 2021; Accepted 29 March 2021
Available online 3 April 2021

2001). In some cases, dermal light sensitivity has been confirmed from behavioural responses, mediated by light intensity and wavelength (Desmond Ramirez et al., 2011). For example the larvae of *Tenebrio molitor* avoid light even after decapitation (Tucolesco, 1933). Light sensitivity of the *Aphis fabae* antennae is responsible for the insect's photokinetic activity (Booth, 1963).

Here we highlight the specific architecture of *Morimus asper funereus* (Mulsant, 1863) (Insecta: Coleoptera: Cerambycidae) elytra, which implicates dermal detection of IR radiation, a feature not previously observed in any other species. We also study the radiative properties of the elytra. Electron and optical microscopy were used to reveal the external and internal morphology of elytra, and thermal imaging to establish its radiative properties in the thermal IR (7.5–13 μm) part of the spectrum. Theoretical analysis and 3D modelling were used to reveal the role of microstructures.

2. Materials and methods

2.1. Insect

Morimus asper funereus (Fig. 1) (family Cerambycidae, subfamily Lamiinae) is a large longicorn beetle inhabiting central and southern Europe. The species is characterized by grey elytra with four black patches and a body length of 15–40 mm (Parisi and Busetto, 1992). The colouration and velvety appearance of the elytra comes from the dense tomentum of the setae, grey hairs and black scales, embedded in the elytral surface, which is black and shiny. The hind wings (alae) of *M. asper funereus* are reduced and the species is flightless (Solano et al., 2013).

M. asper funereus is a saproxylic species (Carpaneto et al., 2015; Hardersen et al., 2017) and depends on decaying wood during larval development. This process takes place in tree trunks and stumps and lasts approximately three or four years (Stanić et al., 1985). We noticed that the insects evade direct sunlight. We never found them on trunks that were directly exposed to solar radiation: when we subjected an insect to sunlight, it hid in the shadow. This was confirmed by other research, which found that this species is active during the evening and at night (Polak and Maja, 2012; Romero-Samper and Bahülo, 1993). Hardersen et al. (2017) determined that the highest activity of the species was between 20:00 and 24:00. However, the authors stated that *M. asper funereus* individuals were seen during the day, but that the number was only 30% of the maximum recorded in the evening and at night.

The species is strictly protected in Europe (and Serbia) by Annex II of the Habitat Directive 92/43/CEE. In the IUCN Red List of Threatened Species, it is designated as vulnerable (A1c) (IUCN Red List of Threatened Species, 2018). We had ten, conserved and pinned, specimens at our disposal, collected during the summer of 2018 on Mt. Avala, near the city of Belgrade, with the permission of the Serbian Ministry of Environmental Protection (N°:353-01 –1310/2018-04).

Fig. 1. *Morismus asper funereus*: a longicorn beetle whose most prominent features are black body and greyish elytra with four prominent black patches.

2.2. Microanalysis

A stereomicroscope (STEBA600, Colo Lab Experts, Slovenia) with maximum magnification up to 180X, eyepiece 20X, auxiliary objective 2X, working distance 100 mm, reflection and transmission mode, and equipped with a digital camera (Canon EOS 50D, Tokyo, Japan) was used to examine the anatomy of the whole insect.

The optical characteristics of the elytra and setae were analysed on a trinocular microscope (MET104, Colo Lab Experts, Slovenia) (maximum magnification 400X, polarization set, objectives Plan Achromatic POL Polarizing 10X/20X/40X).

Micro-computed tomography (micro-CT) was employed to view the overall anatomy of the beetle and measure the thickness of the elytra. We had at our disposal the Skyscan 1172 system (Bruker, USA). To ensure the optimum signal/noise ratio during micro-CT imaging, the specimens were scanned without filter, with scanning parameters set as follows: 40 kV, 244 μA, 530 ms, rotation step 0.2° (pixel size 13.5 μm). For the purpose of this experiment, CT scanning was performed without any special preparation of a specimen.

A field emission gun scanning electron microscope (FEGSEM) (MiraSystem, TESCAN, Czech Republic) was used for ultrastructural analysis. Prior to analysis, insect elytra were removed and placed on an aluminium mount and coated with a thin layer (5–10 nm) of gold palladium (AuPd), using a SC7620 Mini Sputter Coater (Quorum Technologies Ltd., UK).

2.3. Thermal infrared (IR) analysis

Assessment of the thermal properties of insects is normally done by some kind of thermometry (Heinrich, 2013). With the advent of IR cameras, thermal imaging (TI) becomes a method of choice. It is a non-invasive and non-contact technique with applications in numerous fields (Vollmer and Möllmann, 2010). Recently, TI become an important sensing technology in biological investigations (Kastberger and Stachl, 2003). TI cameras are a relatively new tool in studying nocturnal flying animals: birds, bats and insects (Horton et al., 2015). So far, most TI studies of insects have focused on the thermoregulation of Hymenoptera species (Stabentheiner and Schmaranzer, 1987; Stabentheiner et al., 2012).

In this research, the emission of thermal radiation was analysed by an IR thermal camera corresponding to an atmospheric window at 7.5–13 μm (FLIR A65, USA, 640 x 512 pixels, thermal resolution/NETD 50 mK). Thermal measurements were corrected for surface emissivity, and reflected temperature, while images were acquired without binning. Due to the smallness of the insect, we positioned the camera as close as possible (at a distance between 10 and 20 cm), and sometimes used an additional lens to further magnify the thermal image. Under these conditions, the Narcissus effect (radiation emitted by the camera itself) was pronounced. For this reason, we positioned the elytra outside the thermal beam emanating from the camera objective. The rest of the camera body was shielded by aluminium foil.

We manufactured an aluminium cavity and coated it with an absorbing, velvety material whose absorbance was measured at 0.996, in agreement with the calculated value (Prokhorov, 2012). It was used as a reference to measure elytra emissivities, as shown in Fig. 2.

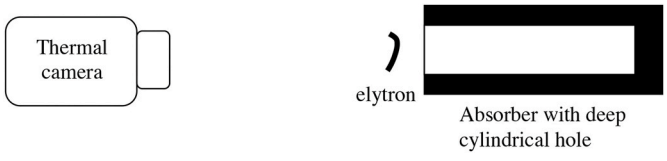

Fig. 2. A simple experimental setup for thermal measurements.

3. Results

3.1. Morphological and optical characterization of photonic structures of *M. asper funereus*

The macroscopic anatomy of a dried specimen, visualized using micro-CT (Fig. 3), showed that the elytra of *M. asper funereus* are ellipsoidal, sclerotized and thick (between 200 and 350 μm). The hind wings of *M. asper funereus* are highly reduced and there is a large, air-filled space between the elytra and the insect body.

The elytra of *M. asper funereus* (Fig. 1) possess a hierarchical structure with a number of features ranging from macroscopic to micron and submicron levels.

The inner surface (facing the insect body) looks spongy (Fig. 4(a)), with an array of oval zones (approx. 0.2–0.4 mm in size – see Fig. 4(b)), surrounded by yellowish walls. If observed in transmission, it can be seen that the walls are actually a complex, connected network of channels that transport hemolymph (Fig. 4(c)) (Unruh and Chauvin, 1993; van de Kamp and Greven, 2010). Within each zone, there is a spherical-looking object with a circular opening at its centre that looks like a standard blackbody (BB) model found in textbooks. In transmission (Fig. 4(c)), BBs are deep red, doughnut-shaped features in the middle of each oval zone. It should be noted that the red colour is due to melanin, characterized by strong absorption in the blue-green part of the spectrum and good transmission in the red. By bleaching elytra using hydrogen peroxide (H_2O_2) we were able to reveal a network of smaller channels, connecting the BB to the main microfluidic channels. (Fig. 4(d)).

All the structures described above are protected by an optically transparent layer. This layer is electron-dense (Fig. 5) and hides all the structures observed optically. Microtrichia (thorn-like structures, approx. 5 μm in height – inset in Fig. 5) are a dominant feature of the internal surface. As can be seen, the microtrichia are arranged in an ordered but not completely regular pattern (average mutual distance is 11 μm). In many other insects, such structures are used to lock the hind wings to the elytra, as in the Asian ladybeetle (Sun et al., 2018).

Outer surface of elytra is black and covered with two different types of microtrichiae (Fig. 6(a) and (b)). One type is transparent and covers most of the body, which looks greyish (grey zone) due to the scattered radiation. The other type is pigmented and densely covers four distinct areas producing characteristic black patches. However, in thermal infrared, the whole body looks quite uniform.

On grey elytral zone there is also an array of shiny black, quite smooth, microlens-like protrusions, surrounded with hairs (compare optical and SEM images in Fig. 6(c), respectively). The microlenses and BBs have a well-defined mutual orientation, which was observed by simultaneously illuminating the elytron in transmission and reflection (Fig. 7). As observed before (Fig. 4), the BB occupies the centre of an oval zone, while the microlens is at its rim, directly facing a hemolymph-filled channel.

The elytron directly beneath the surface (procuticle 200-μm thick) is well organized, as in all coleopteran (van de Kamp and Greven, 2010; van de Kamp et al., 2016). It is layered and possesses a number of laminae that envelope the BBs and microchannels (Fig. 8(a)). It is interesting to note a number of tiny hairs covering the internal surface of the blackbody (Fig. 8(b)). At the moment, we can only speculate about their biological function, because this can be revealed only by physiological investigation of live specimens, which we didn't have at our disposal. However, from purely physical point of view, we note that hairs increase the absorbance of the black body wall due to enhanced scattering and trapping of radiation.

3.2. Radiative properties of *M. asper funereus*

We used thermal imaging to evaluate radiative properties of elytra. An elytron was placed in front of the reference cavity (with absorbance higher than 99% (Prokhorov, 2012)) and observed with a thermal camera (operating within the 8–14 μm wavelength range). In thermal equilibrium (room temperature), the elytron completely disappears from thermal image (Fig. 9(a)) and becomes visible only when heated by the laser beam (Fig. 9(b)). The same is true for both the outer and inner sides, along the entire, highly curved, elytral surface. Thus, we may conclude that the high directional emissivity (higher than 99%) is constant along the surface and has the characteristics of a Lambertian source.

It is interesting to note that the emissivity of both black and grey areas of elytra is the same. This is because the wavelength of thermal radiation is close to characteristic dimensions of hairs covering the

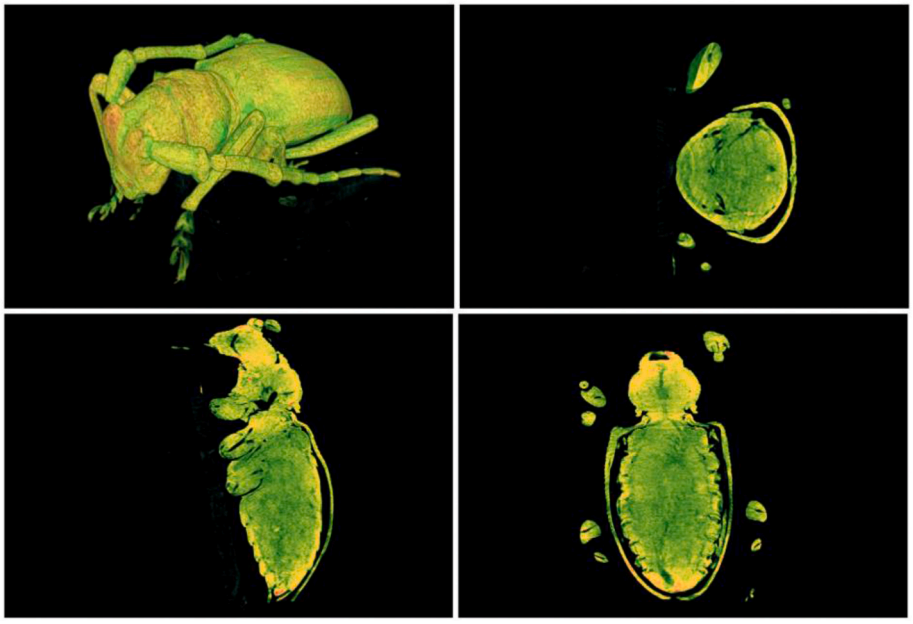

Fig. 3. (a)3D reconstruction of *M. asper funereus* from a stack of MictoCT images. (b) frontal, (c)axial and (d) longitudinal cross sections of insect showing air filled space between elytra and the rest of the body.

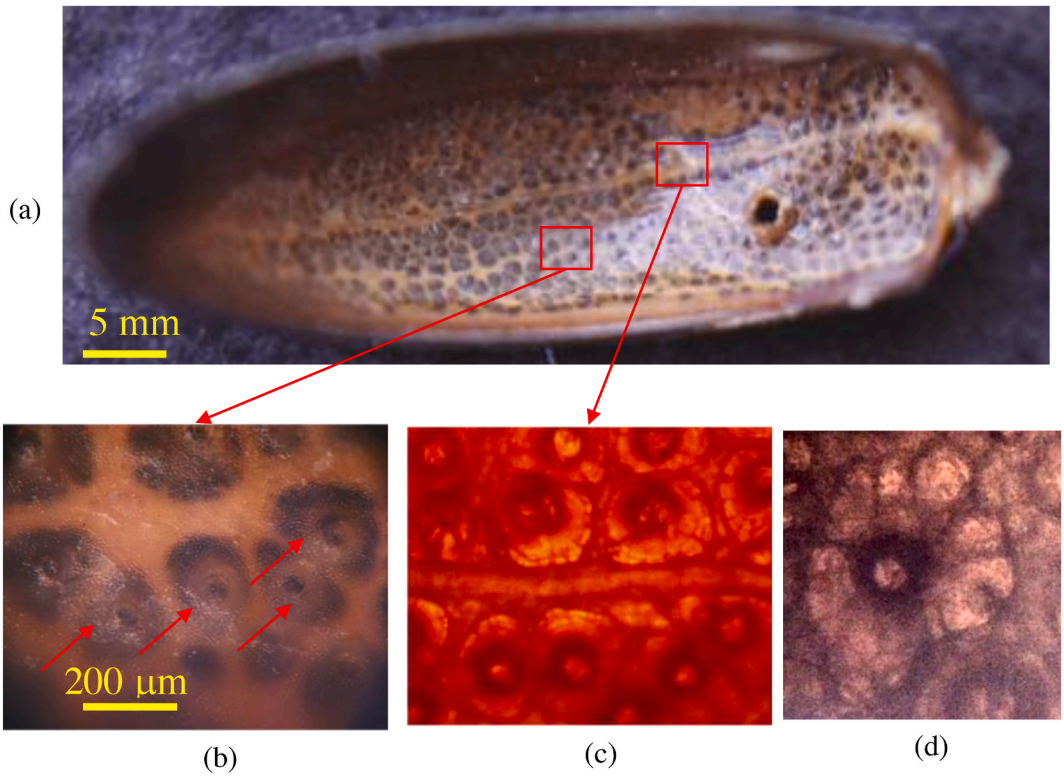

Fig. 4. (a) Optical image of inner elytral surface of *M. asper funereus* in its natural state, exhibiting its original pigmentation. Enlarged portion in (b) shows blackbody-like (BB) structures (spherical-looking, with a black spot in the centre – red arrows). (c) Transmission optical image of elytron reveals a system of channels, branching from the central channel and surrounding each BB. (d) Elytron bleached in peroxide reveals a network of smaller channels, connecting the BB to the main microfluidic channels.

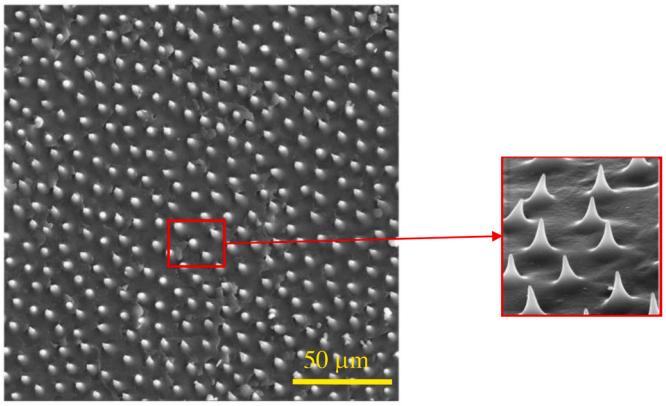

Fig. 5. SEM image of inner elytral surface of *M. asper funereus* with an array of microtrichia, enlarged in the inset.

elytra. That is why both types of hairs efficiently scatter the radiation and enhance the probability of radiation being absorbed.

3.3. Modelling of *M. asper funereus* elytron

3.3.1. Blackbody array

Based on the anatomical features described in section 3.1, we were able to design a model of *M. asper funereus*. We took the oval zone of Fig. 4 as an elementary unit, composed of a layered blackbody surrounded by walls with microchannels. Blackbody is enclosed between two layers, one containing microlenses and the other covered by microtrichia.

We used 3D, open-source, computer graphics software (Blender, free under GPL) to visualize the elementary unit of *M. asper funereus* elytra. Fig. 10(a) and (b) show two aspects of an elementary cell, so that the spatial relations between the microlenses, walls with microchannels and blackbody are clearly seen. Microlenses focus radiation directly into the elytron and microchannel filled with hemolymph (primarily water), as confirmed by ray tracing (Fig. 11) within a quite large angular range (−20° to +20°).

We made a more exact finite element modelling of IR wave propagation in the cuticle. To do that, we needed complex refractive indices of chemolimph and insect cuticle at thermal infrared wavelengths. Chemolimph is mostly composed of water and we used the data from Hale and Querry (1973) – complex refractive index was averaged to $n = 1.2 + i \cdot 0.0343$, within 3–5 μm, and $n = 1.35 + i \cdot 0.13$, within 8–12 μm. Optical constants of insect cuticle at thermal infrared are not very well known and we used data extracted from Shi (2018) – within 3–5 μm complex refractive index was $n = 1.57 + i \cdot 0.005$ and within 8–12 μm, $n = 1.57 + i \cdot 0.1$. The absorption of melanin was not taken into account because it is found only in a thin superficial layer of elytra, its concentration is low, compared to that of chitin, and its absorption maximum is at UV.

Within the 8–12 μm window, radiation is efficiently absorbed in the superficial layers of the cuticle due to the very high absorption coefficient of chitin (see Fig. 12(b)). The situation is more interesting within the 3–5 μm window, where the absorption as an order of magnitude lower (Shi, 2018). There, the radiation is indeed focused onto the microchannels (Fig. 12(c)), while the multilayer structure of the BB efficiently reflects and expels the radiation from the central cavity. Within this spectral range, radiation penetrates deep and heats the internal structures of cuticle (Fig. 12 (c)). If there is a constant flow of hemolyph through the cuticle (Unruh and Chauvin, 1993) heat will be convectively transferred to the central cavity of the blackbody. That is why we propose that tiny hairs lining the cavity might function as

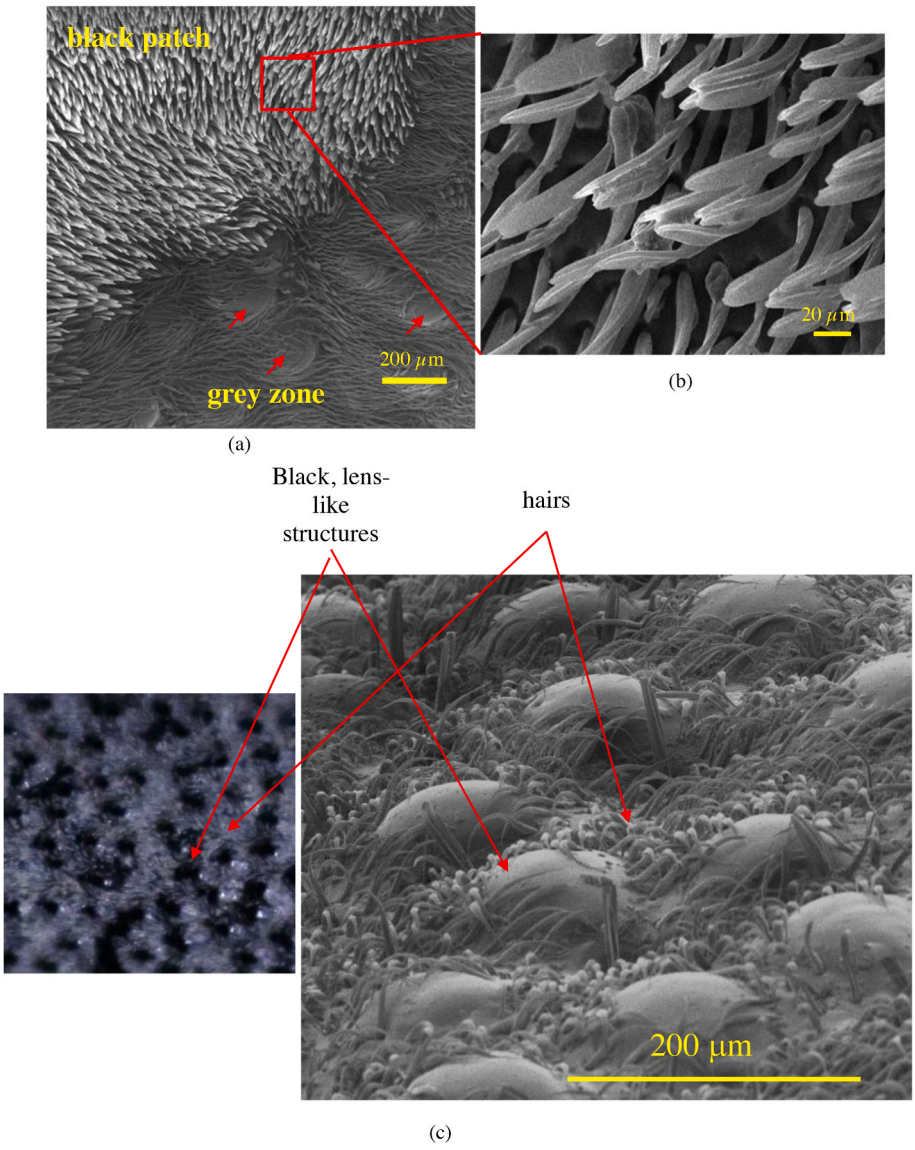

Fig. 6. SEM of the outer surface of the *M. asper funereus* elytra: (a) an edge between grey and black areas (red arrows indicate microlens-like protrusions); (b) enlarged SEM image of black scales. (c) Lens-like structures and hairs on the outer surface of *M. asper funereus*. Optical image is on the left and SEM image on the right. The captured area with lens-like structures is from the grey zone of the elytra.

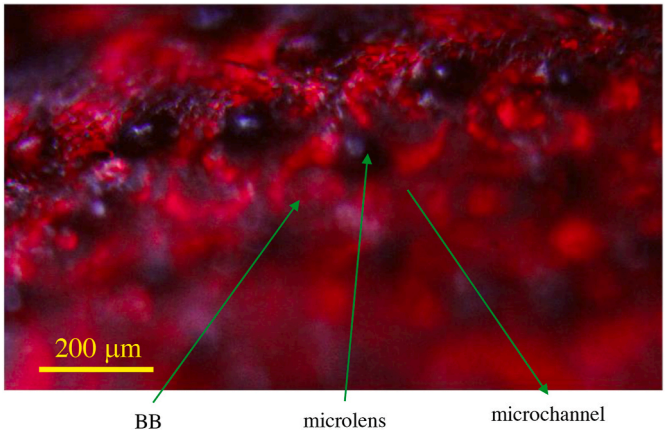

Fig. 7. Optical microscope image of elytron, simultaneously illuminated in reflection and transmission. Microlenses can be seen as black circular areas, blackbodies are doughnut-shaped zones within the network of channels.

sensilla, signalling the insect to search for a cooler place - which is a behavioural characteristic of this particular insect.

It seems that cuticular microlenses function like the cornea of an ommatidium, i.e. they focus radiation onto the sensitive layer. The architecture of *M. asper funereus* is well organized for the purpose.

3.3.2. *Array of microtrichia*

As can be seen from micro-CT images (Fig. 3), there is a thin (less than a millimetre) air-filled gap between the elytra and the insect body (see scheme at Fig. 13). Thermal energy is radiatively exchanged between those layers, thus filling the gap with infrared radiation. For the part of radiative energy propagating at grazing incidence, gap behaves as a hollow waveguide (such as those used for 10.6 μm CO_2 lasers – (Komachi et al., 2000)) with microtrichie as subwavelength scattering (diffractive) structures. In such waveguides, radiation propagates in a whispering-gallery manner.

In the following we will analyze their possible role in thermal radiation exchange of *M. asper funereus*. For the purpose of better understanding, we will treat microtrichie as a forest-like structure of almost conical protuberances on an otherwise flat surface. Each cone is 4.4 μm

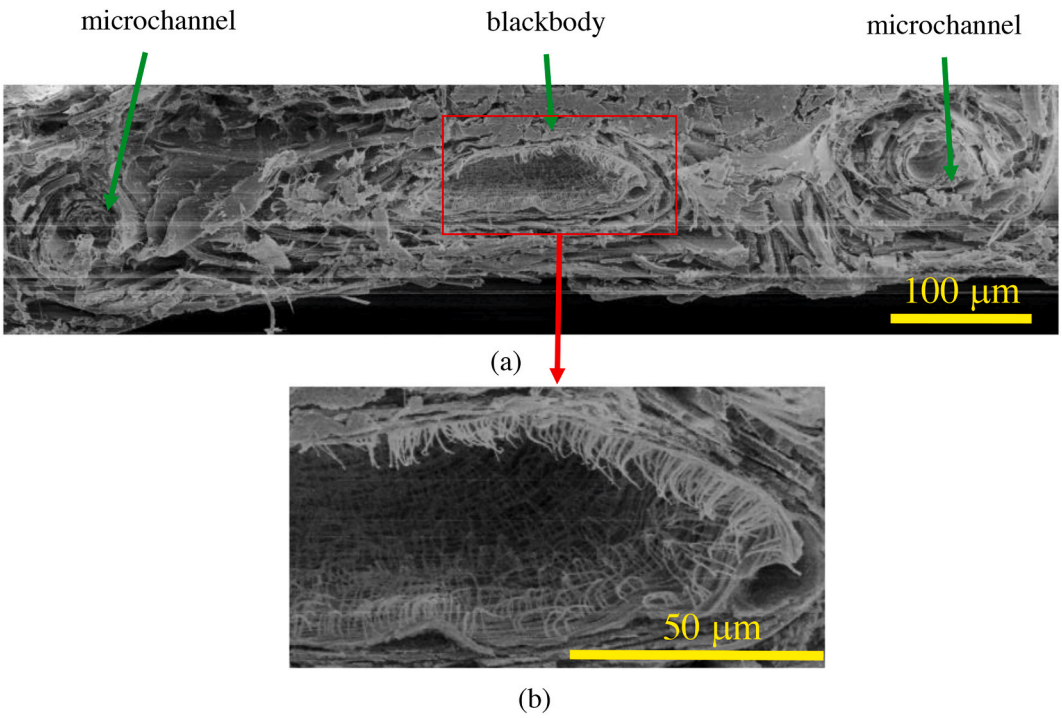

Fig. 8. (a) Cross section of *M. asper funereus* elytron with clearly visible blackbody with microchannels on both sides. (b) Enlarged image reveals the hair-like protrusions lining the internal surface of the blackbody.

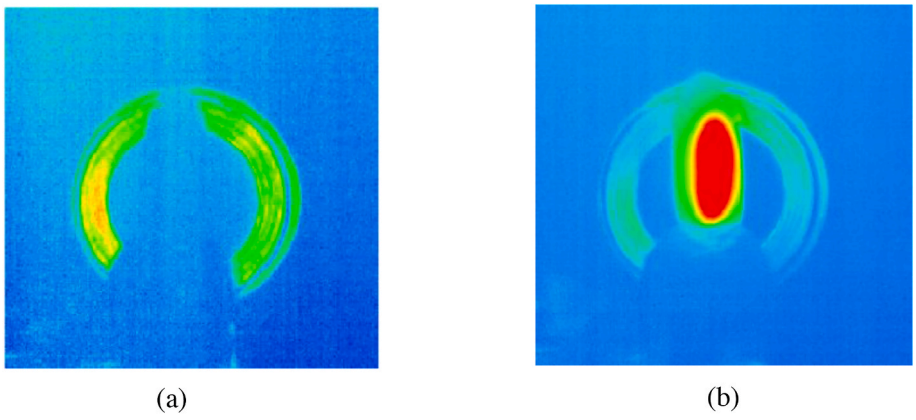

Fig. 9. (a) Thermal image of *M. asper funereus* elytra positioned in front of a blackbody. Emissivity is the same and they cannot be discerned. (b) When heated, the elytron becomes visible.

in diameter at its base and 3.8 μm in height. An observer looking from above will see an arrangement like that in Fig. 14, schematically drawn using the section of Fig. 5 as a template. Looking from the side, as if sitting on the substrate, densely overlapping cone projections, even for a small number of microtrichia surrounding the central one, are observed. Thus, for the large number of microtrichia on the elytron, the radiation propagating close to the surface has a high chance of hitting a cone and being absorbed. This is a purely geometric optic analysis – in the following we will present a wave optics perspective.

Upon closer inspection of the spatial distribution of microtrichia (Fig. 5), we can see that it is neither regular nor completely random (rods in the chicken retina are arranged in a similar fashion (Jiao et al., 2014)). It is characterized by a ring-like Fourier transform, as in Fig. 15 (a). The spatial frequency of the prominent ring-like structure is 0.1/μm, corresponding to the average 10-μm distance between microtrichia (Fig. 15(b)). The amplitude of the Fourier transform goes to zero as the spatial frequencies approach the central Fourier peak. This is a characteristic of hyperuniform point distributions, which were shown to behave as a complete photonic bandgap structure (Florescu et al., 2009). The slight ellipticity of the Fourier transform observed here is possibly a consequence of the ellipsoidal profile of the elytron.

For thermal radiation entrapped between the elytra and the body, A 2-dimensional hyperuniform system behaves as a random full-bandgap photonic crystal. This can be inferred from the ring-like Fourier transform (Fig. 15(a)), which can be understood as a superposition of sinusoidal gratings with a 10-μm period oriented in all directions along the plane substrate. Under grazing incidence, gratings behave as Bragg reflectors, blocking the propagation of radiation with the wavelength:

$$\lambda = 2d/N$$

where d is a grating period, N is an integer, assuming the normal angle of incidence. For the 10 μm average period of microtrichia and $N = 2$, the Bragg wavelength is 10 μm, right in the middle of an 8–12 μm atmospheric window. Additionally, for N = 4, the Bragg wavelength

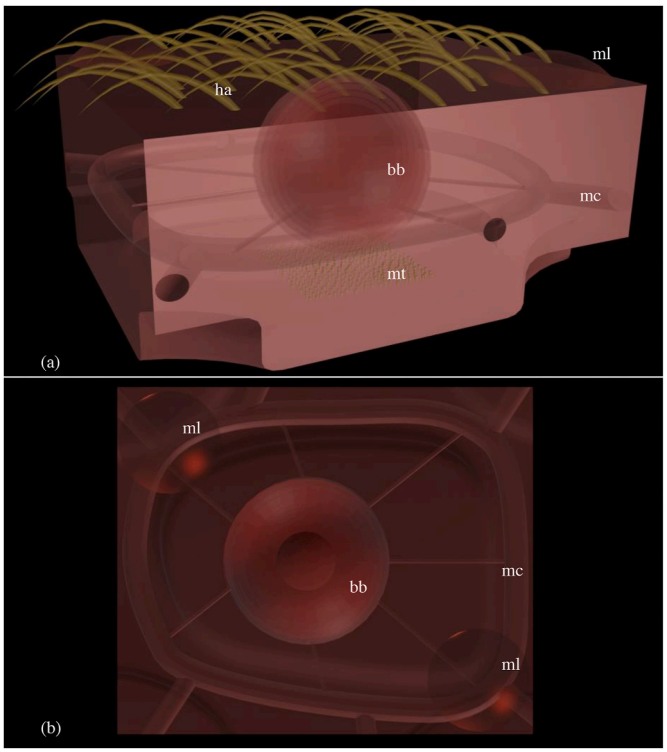

Fig. 10. (a) A semi-transparent 3D model of *M. asper funereus* elytron presenting internal structures hidden within the elytron (mt – microtrichia, mc – microchannels, ml – microlens, bb – black body, ha – hairs) (a) with microlenses and hairs clearly seen; (b) top view displaying alignment of microlenses and microchannels. The microchannel completely surrounds the blackbody and is connected to it via even smaller channels.

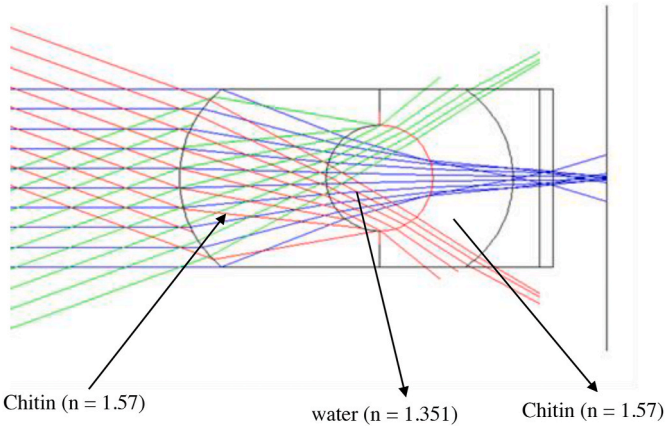

Fig. 11. Ray tracing through a microlens and microchannel (blue rays are incoming at normal incidence, while red and green rays obliquely, at $+20^0$ and -20^0, illuminate the elytron). Calculations were done at 3 μm, where refractive indices are as indicated in figure.

corresponds to another window at 3–5 μm, but we were not able to check this experimentally.

4. Discussion and conclusions

The search for highly absorbing structures is a long-standing one and many structured materials have been engineered so far (Mizuno et al., 2009), but only the vertically aligned nanotube array (VANTA black) (De Nicola et al., 2017) approaches the emissivity of a blackbody. In line with the research on silicon photonics for NIR silicon devices (Milošević et al., 2019), here we show that natural, less complex structures can achieve similar results owing to their forest-like structure and intrinsic curvature (Leonhardt and Tyc, 2009). A clever arrangement of hyperuniform disordered structures efficiently competes with highly advanced nanotube structures. In contrast to artificial VANTA black material, which is fragile and complex to manufacture, the natural solution is robust and simple.

At this point, we are not able to estimate how important the role of microtrichie is. We must stress, however, that the amount of the radiation entrapped between elytra and the body is non-negligible due to Fresnel reflections and waveguiding. Simple calculation shows that, for the refractive index used in this study (n = 1.57) and normal incidence,

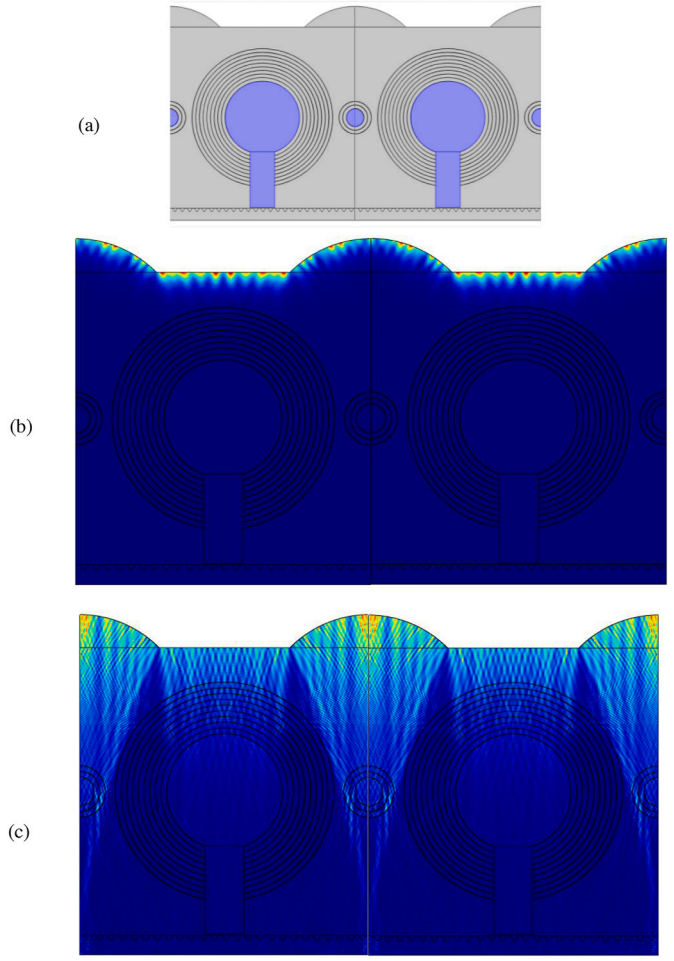

Fig. 12. (a) A model of *M. asper funereus* elytron used in FEM analysis (grey colour corresponds to chitin and purple to water). Distribution of thermal IR radiation inside *M. asper funereus* blackbody-like cuticular structure calculated by FEM. Two spectral windows were analysed: (b) 8–12 μm (image at 10 μm is shown) and (c) 3–5 μm (image at 4 μm is shown).

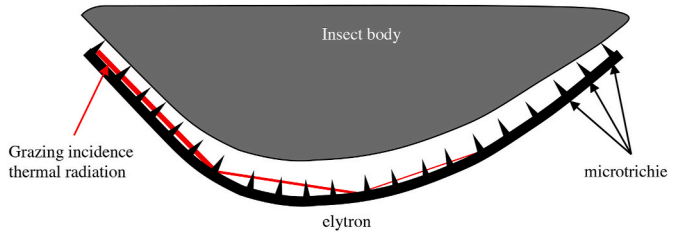

Fig. 13. M. funereus elytron and body with air filled gap acting as a hollow waveguide for grazing incidence thermal radiation.

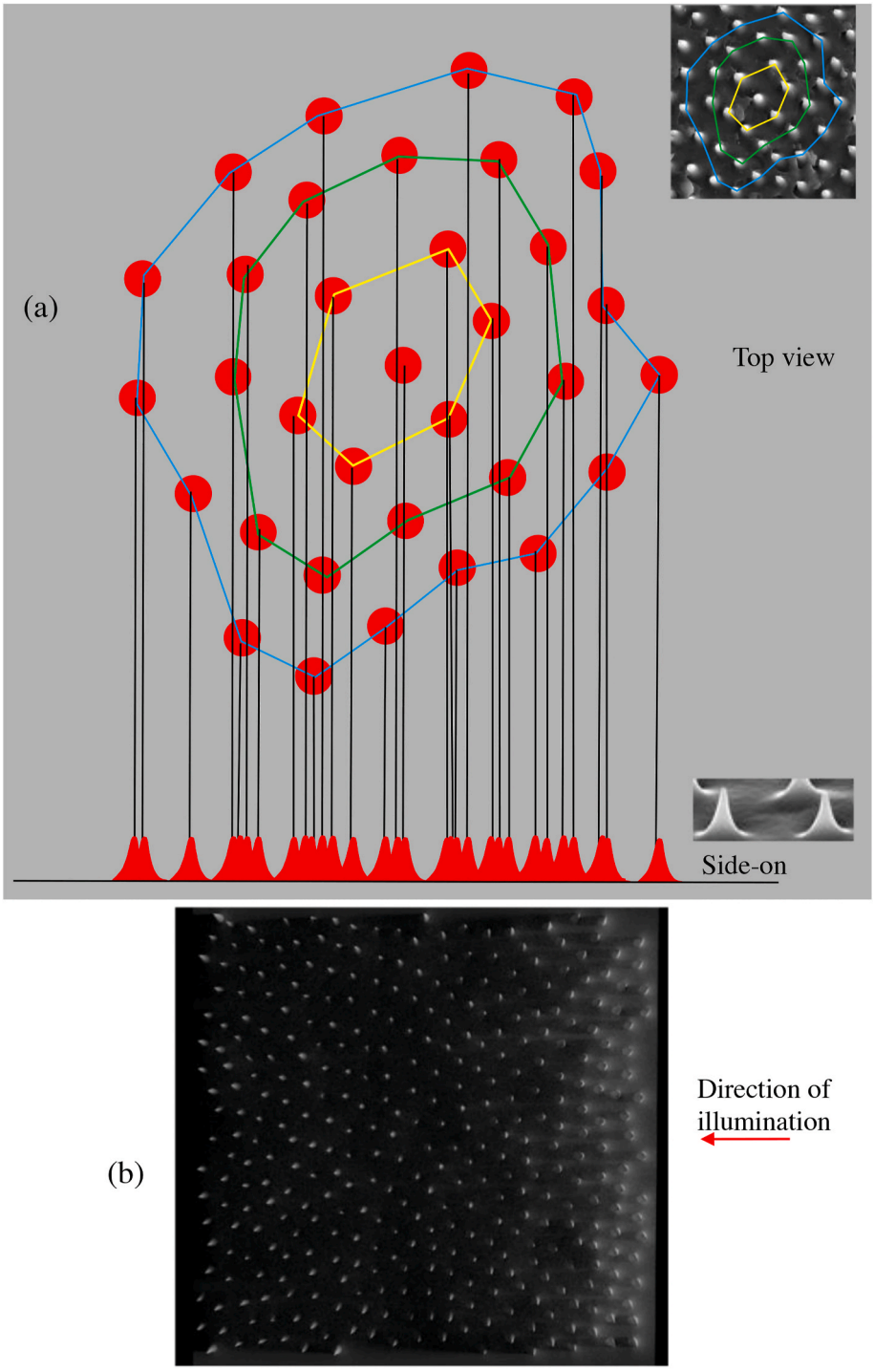

Fig. 14. (a) An arrangement of conical structures seen from above and drawn using Fig. 2 as a template. Inset in the upper right corner shows part of the SEM image used as a template. Side-on view is shown at the bottom of this figure. (b) Top view of a microtrichia 3D model illuminated obliquely from the right (red arrow) shows that microtrichia preclude the propagation of light.

4.99% of radiation is reflected, while for grazing incidence almost all radiation is reflected. Between those two extremes, due to uniform angular distribution of thermal radiation, it is clear that more than 4.99% of thermal radiation is entrapped and waveguided between body and elytra. More detailed answer to this question will be given in further studies.

In the interests of brevity and focus, several other elytral features that might be effective in thermal IR had to be left out of the scope of this paper. First of all, the chitinous lamellae of *M. asper funereus* have a characteristic dimension of 4–5 μm with the corresponding Bragg wavelength of 8–10 μm. Each layer contains well-oriented microfibrils that certainly introduce birefringence, and the orientation of microfibrils is different in each layer (Supplement file). The exact value of the refractive index of chitinous structures is not very well known, in particular in the thermal infrared, and it is therefore difficult to make the correct theoretical calculations and numerical simulations. Thirdly, interfaces between each layer are rough and scatter radiation, so that the layers may act as planar waveguides to additionally absorb the

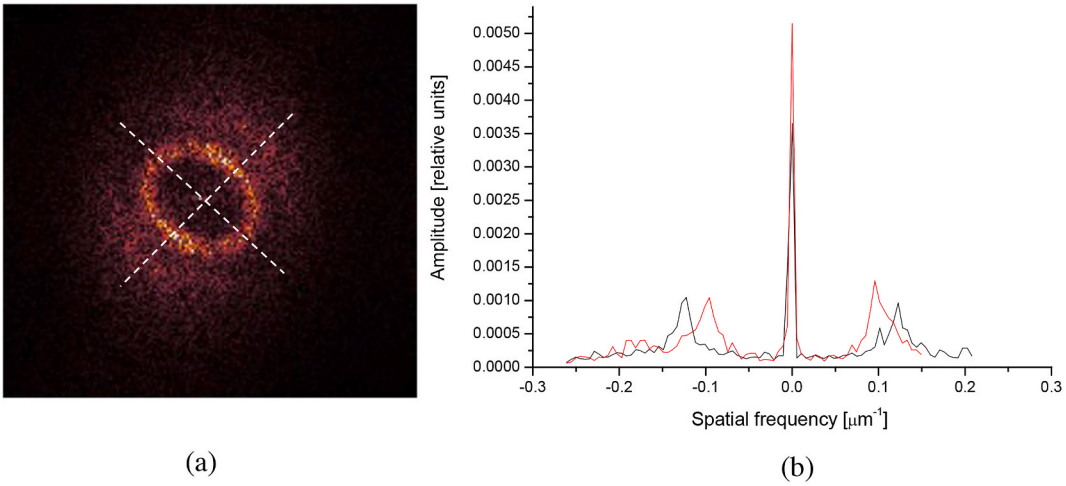

Fig. 15. (a) A Fourier transform of the image in Fig. 2 depicting the arrangement of microtrichia. Note the ring-like pattern with slight ellipticity. (b) Scanning along two orthogonal directions (see dotted lines in (a)) shows a pronounced peak at spatial frequency close to 0.1/μm, corresponding to the average 10-μm distance between microtrichia.

radiation. Finally, microtrichia can act as transmission gratings for non-obliquely impinging radiation and diffraction orders can be coupled into layers as planar waveguides.

From a theoretical point of view, it is quite difficult to treat inherently random structures (such as those of *M. asper funereus*) using exact methods like FEM, RCWA or FDTD. For large structures, periodic boundary conditions have to be introduced, thereby violating inherent randomness. If a random structure is to be simulated, computer memory requirements become extremely large and computational time intolerably long.

We performed other measurements that have revealed the excellent thermal insulation properties of this particular insect. By laser-heating one side of an elytron we observed that, in thermal equilibrium, the other side was approximately 20 °C lower in temperature. It is difficult to discern the contribution of radiative dissipation, with respect to other processes (convection and conduction) (Supplement file). However, the *M. asper funereus* elytron could be an excellent model to design similar thermally insulating materials.

Furthermore, taking into account that *M. asper funereus* lays its eggs in and emerging larvae feed on decaying wood (a saproxylic way of life), similarly to pyrophilous insects (Klocke et al., 2011), it is important for an insect to detect dead trees. Thermal fingerprint of a decaying wood is different, compared to healthy specimens, primarily due to the reduced amount of water. (Pitarma et al., 2019). Based on the structures and properties we have observed, we postulate that a number of infrared detectors on the elytron is used to detect the infrared fingerprint of wood and discriminate between healthy and decaying tree trunks. Even though the number of elytral IR detectors (approx. 400) is small, it is still a useable one, if compared to that of FLIR ONE Gen3 smart-phone, clip-on thermal cameras (60 x 80 IR pixels). By making this comparison we emphasize the "ingenuity" of evolution, in no way endorsing any particular IR camera.

It is well known that Coleoptera elytron has a complex layered structure with number of cavities, trabeculae, channels and pores (Sun and Bhushan, 2012). Research mostly dealt with mechanical significance of internal architecture of elytron (Du and Hao, 2018), and to a lesser degree with thermal effects (Le et al., 2019). By studying available literature we may say that many of structures might serve similar role in thermal radiation management, due to their characteristic dimensions being close to the wavelength of thermal radiation.

In conclusion, we have shown that a combination of micron-sized blackbodies and uniformly random microstructures possesses excellent properties to manage thermal radiation. The range of potential applications is enormous and even might even extend from NIR to terahertz technology.

Funding

This work was supported by the Serbian Ministry of Education, Science and Technological Development, and the Science and Technology Development Programme – Joint Funding of Development and Research Projects of the Republic of Serbia and the People's Republic of China: Mimetics of insects for sensing and security, No. I-2. BK acknowledges support from the F.R.S.- FNRS. DP acknowledges support from L'Oréal-UNESCO"For Women in Science".

Ethical approval

All necessary permissions to collect the samples of *M. asper funereus* were obtained from the Ministry of Environmental Protection of the Republic of Serbia and the Institute for Nature Conservation of Serbia. The research did not include live insects.

Author statement

Darko Vasiljević : Formal analysis, Data Curation, Visualization.
Danica Pavlović: Conceptualization, Formal analysis, Investigation, Resources, Writing-Original Draft Preparation.
Vladimir Lazović: Formal analysis.
Branko Kolarić: Project Administration, Writing Review and Editing.
Branislav Salatić: Softwer, Formal analysis.
Wang Zhang: Supervision, Validation.
Di Zhang: Supervision, Validation.
Dejan Pantelić: Conceptualization, Methodology, Investigation, Formal analysis, Writing-Original Draft Preparation.

Declaration of competing interest

The authors declare no conflict of interest.

Appendix A. Supplementary data

Supplementary data to this article can be found online at https://doi.org/10.1016/j.jtherbio.2021.102932.

References

Arikawa, K., Takagi, N., 2001. Genital photoreceptors have crucial role in oviposition in Japanese yellow swallowtail butterfly, Papilio xuthus. Zool. Sci. 18 (2), 175–179. https://doi.org/10.2108/zsj.18.175.

Booth, C.O., 1963. Photocinetic function of aphid antennae. Nature 197, 265–266.

Bosi, S.G., Hayes, J., Large, M.C.J., Poladian, L., 2008. Color, iridescence, and thermoregulation in Lepidoptera. Appl. Opt. 47, 5235–5241. https://doi.org/10.1364/AO.47.005235.

Capinera, J.L., 2008. Encyclopedia of Entomology. Springer, New York.

Carpaneto, G.M., Baviera, C., Biscaccianti, A.B., Brandmayr, P., Mazzei, A., Mason, F., Battistoni, A., Teofili, C., Rondinini, C., Fattorini, S., Audisio, P., 2015. A Red List of Italian Saproxylic Beetles: taxonomic overview, ecological features and conservation issues (Coleoptera). Fragm. Entomol. 47, 53. https://doi.org/10.4081/fe.2015.138.

Cossins, A., 2012. Temperature Biology of Animals. Springer Science & Business Media.

De Nicola, F., Hines, P., De Crescenzi, M., Motta, N., 2017. Thin randomly aligned hierarchical carbon nanotube arrays as ultrablack metamaterials. Phys. Rev. B 96 (4), 045409. https://doi.org/10.1103/PhysRevB.96.045409.

Desmond Ramirez, M., Speiser, D.I., Sabrina Pankey, M., Oakley, T.H., 2011. Understanding the dermal light sense in the context of integrative photoreceptor cell biology. Vis. Neurosci. 28, 265–279. https://doi.org/10.1017/S0952523811000150.

Doucet, S.M., Meadows, M.G., 2009. Iridescence: a functional perspective. J. R. Soc. Interface 6 (Suppl. l_2), S115–S132. https://doi.org/10.1098/rsif.2008.0395.focus.

Du, J., Hao, P., 2018. Investigation on microstructure of beetle elytra and energy absorption properties of bio-inspired honeycomb thin-walled structure under axial dynamic crushing. Nanomaterials 8 (9), 667. https://doi.org/10.3390/nano8090667.

Florescu, M., Torquato, S., Steinhardt, P.J., 2009. Designer disordered materials with large, complete photonic band gaps. Proc. Natl. Acad. Sci. Unit. States Am. 106 (49), 20658–20663. https://doi.org/10.1073/pnas.0907744106.

Gillott, C., 2005. Food uptake and utilization. Entomology (Tokyo) 487–513. https://doi.org/10.1007/1-4020-3183-1_16.

Gullan, P.J., Cranston, P.S., 2004. The Insects: an Outline of Entomology. John Wiley & Sons.

Hale, G.M., Querry, M.R., 1973. Optical constants of water in the 200-nm to 200-μm wavelength region. Appl. Opt. 12 (3), 555–563. https://doi.org/10.1364/ao.12.000555.

Hardersen, S., Bardiani, M., Chiari, S., Maura, M., Maurizi, E., Roversi, P.F., Mason, F., Bologna, M.A., 2017. Guidelines for the monitoring of Morimus asper funereus and Morimus asper asper. Nat. Conserv. 20, 205–236. https://doi.org/10.3897/natureconservation.20.12676.

Heinrich, B., 2013. The Hot-Blooded Insects: Strategies and Mechanisms of Thermoregulation. Springer Science & Business Media, New York.

Horton, K.G., Shriver, W.G., Buler, J.J., 2015. A comparison of traffic estimates of nocturnal flying animals using radar, thermal imaging, and acoustic recording. Ecol. Appl. 25 (2), 390–401. https://doi.org/10.1890/14-0279.1.sm.

Jiao, Y., Lau, T., Hatzikirou, H., Corbo, J.C., Torquato, S., Mathematics, A., 2014. Avian photoreceptor patterns represent a disordered hyperuniform solution to a multiscale packing. Phys. Rev. 89 (2), 022721 https://doi.org/10.1103/PhysRevE.89.022721. Avian.

Kastberger, G., Stachl, R., 2003. Infrared imaging technologies. Behav. Res. Methods Instrum. Comput. 35 (3), 429–439.

Kemp, D.J., 2007. Female butterflies prefer males bearing bright iridescent ornamentation. Proc. Biol. Sci. 274 (1613), 1043–1047. https://doi.org/10.1098/rspb.2006.0043.

Kingsolver, J.G., 1985. Butterfly thermoregulation: organismic. J. Res. Lepid. 24 (1), 1–20.

Klocke, D., Schmitz, A., Soltner, H., Bousack, H., Schmitz, H., 2011. Infrared receptors in pyrophilous ("fire loving") insects as model for new un-cooled infrared sensors. Beilstein J. Nanotechnol. 2 (1), 186–197. https://doi.org/10.3762/bjnano.2.22.

Komachi, Y., Wakaki, M., Kanai, G., 2000. Fabrication of hollow waveguides for CO_2 lasers. Appl. Opt. 39 (10), 1555–1560. https://doi.org/10.1364/ao.39.001555.

Le, V.T., Ha, N.S., Goo, N.S., 2019. Thermal protective properties of the allomyrina dichotoma beetle forewing for thermal protection systems. Heat Tran. Eng. 40, 1539–1549. https://doi.org/10.1080/01457632.2018.1474603.

Leonhardt, U., Tyc, T., 2009. Broadband invisibility by non-Euclidean cloaking. Science 323 (5910), 110–112. https://doi.org/10.1126/science.1166332.

Millott, N., 1968. The dermal light sense. In: Symp. Zool.Soc. London, pp. 1–36.

Milošević, M.M., Man, W., Nahal, G., Steinhardt, P.J., Torquato, S., Chaikin, P.M., Amoah, T., Yu, B., Mullen, R.A., Florescu, M., 2019. Hyperuniform disordered waveguides and devices for near infrared silicon photonics. Sci. Rep. 9 (1), 1–11. https://doi.org/10.1038/s41598-019-56692-5.

Mizuno, K., Ishii, J., Kishida, H., Hayamizu, Y., Yasuda, S., Futaba, D.N., Yumura, M., Hata, K., 2009. A black body absorber from vertically aligned single-walled carbon nanotubes. Proc. Natl. Acad. Sci. Unit. States Am. 106 (15), 6044–6047. https://doi.org/10.1073/pnas.0900155106.

Nijhout, H.F., 1991. The Development and Evolution of Butterfly Wing Patterns, vol. 293. Smithson. Inst. Sch. Press.

Parisi, V., Busetto, A., 1992. Revisione dei Coleotteri presenti nella collezione "A. Leosini". Parte 2a. Scarabaeidae, Lucanidae, Cerambycidae. Pubblicazioni del Museo di Storia naturale dell'Università di Parma 5 (1), 1–93.

Pitarma, R., Crisóstomo, J., Ferreira, M.E., 2019. Contribution to trees health assessment using infrared thermography. Agriculture 9 (8), 171. https://doi.org/10.3390/agriculture9080171.

Polak, S., Maja, J., 2012. Phenology and mating behaviour of Morimus funereus (Coleoptera, Cerambycidae). Saproxylic beetles in Europe: monitoring, biology and conservation. Studia Forestalia Slovenica 137, 43–52.

Prokhorov, A., 2012. Effective emissivities of isothermal blackbody cavities calculated by the Monte Carlo method using the three-component bidirectional reflectance distribution function model. Appl. Opt. 51, 2322–2332. https://doi.org/10.1364/AO.51.002322.

Romero-Samper, J., Bahülo, J., 1993. Algunas observaciones sobre la distribución y biología de Morimus asper Cerambycidae en la Península Ibérica. Bol. Asoc. Esp. Entomol. 17, 103–122.

Scoble, M.J., 1992. The Lepidoptera. Form, Function and Diversity. Oxford University Press.

Shi, N.N., 2018. Biological and Bioinspired Photonic Materials for Passive Radiative Cooling and Waveguiding. Doctoral dissertation. Columbia University.

Shi, N.N., Tsai, C.C., Camino, F., Bernard, G.D., Yu, N., Wehner, R., 2015. Keeping cool: enhanced optical reflection and radiative heat dissipation in Saharan silver ants. Science 349 (6245), 298–301. https://doi.org/10.1126/science.aab3564.

Solano, E., Mancini, E., Ciucci, P., Mason, F., Audisio, P., Antonini, G., 2013. The EU protected taxon Morimus funereus Mulsant, 1862 (Coleoptera: Cerambycidae) and its western Palaearctic allies: systematics and conservation outcomes. Conserv. Genet. 14 (3), 683–694. https://doi.org/10.1007/s10592-013-0461-3.

Stabentheiner, S., Schmaranzer, A., 1987. Thermographic determination of body temperatures in honey bees and hornets: calibration and applications. Thermology 2, 563–572.

Stabentheiner, A., Kovac, H., Hetz, S.K., Käfer, H., Stabentheiner, G., 2012. Assessing honeybee and wasp thermoregulation and energetics - new insights by combination of flow-through respirometry with infrared thermography. Thermochim. Acta 534, 77–86. https://doi.org/10.1016/j.tca.2012.02.006.

Stanić, V., Ivanović, J., Janković-Hladni, M., Nenadović, V., Marović, R., 1985. Feeding habits, behavior, oviposition and longevity of the adult cerambycid beetle Morimus asper funereus Muls.(Col., Cerambycidae) under laboratory condition. Acta Entomol. Jugosl. 21, 87–94.

Sun, J., Bhushan, B., 2012. Structure and mechanical properties of beetle wings: a review. RSC Adv. 2 (33), 12606–12623. https://doi.org/10.1039/c2ra21276e.

Sun, J., Liu, C., Bhushan, B., Wu, W., Tong, J., 2018. Effect of microtrichia on the interlocking mechanism in the Asian ladybeetle, Harmonia axyridis (Coleoptera: Coccinellidae). Beilstein J. Nanotechnol. 9 (1), 812–823. https://doi.org/10.3762/bjnano.9.75.

Sweeney, A., Jiggins, C., Johnsen, S., 2003. Polarized light as a butterfly mating signal. Nature 423, 31–32. https://doi.org/10.1038/423031a.

Tucolesco, J., 1933. La dynamique de la larve de *Tenebrio molitor* et la théorie des tropismes. Bull. Biol. 4, 1–35.

Unruh, T.R., Chauvin, R., 1993. Elytral punctures: a rapid, reliable method for marking Colorado potato beetle. Can. Entomol. 125 (1), 55–63.

van de Kamp, T., Greven, H., 2010. On the architecture of beetel elytra. Entomol. Heute 22, 191–204.

van de Kamp, T., Riedel, A., Greven, H., 2016. Micromorphology of the elytral cuticle of beetles, with an emphasis on weevils (Coleoptera: Curculionoidea). Arthropod Struct. Dev. 45 (1), 14–22. https://doi.org/10.1016/j.asd.2015.10.002.

Verstraete, C., Mouchet, S.R., Verbiest, T., Kolaric, B., 2019. Linear and nonlinear optical effects in biophotonic structures using classical and nonclassical light. J. Biophot. 12, 1–13. https://doi.org/10.1002/jbio.201800262.

Vollmer, M., Möllmann, K.P., 2010. Infrared Thermal Imaging: Fundamentals, Research and Applications. John Wiley & Sons.

Vukusic, P., Sambles, J.R., 2003. Photonic structures in biology. Nature 424 (6950), 852–855. https://doi.org/10.1038/nature01941.

Vukusic, P., Sambles, J.R., Lawrence, C.R., Wootton, R.J., 2001. Now you see it - now you don't. Nature 410 (6824). https://doi.org/10.1038/35065161, 36-36.